IMPROVING THE ACCURACY OF LOW COST MEASUREMENT OF DIRECT NORMAL SOLAR IRRADIANCE

Jim Augustyn and Taylor Geer
Augustyn + Company
P.O. Box 7075
Berkeley CA 94707

Tom Stoffel
National Renewable Energy Laboratory
1617 Cole Boulevard
Golden, CO 80401

Frank Vignola and Rich Kessler
Solar Radiation Monitoring Lab
Dept of Physics, U of Oregon
Eugene, OR

Ed Kern and Ruel Little
Schott Applied Power Corporation
4051 Alvis Court
Rocklin, CA 95677

Bill Boyson
Sandia National Laboratories
Albuquerque, NM, U.S.A

ABSTRACT: The accuracy and reliability of direct beam solar irradiance data and measurements are of great importance in the development of concentrating solar power technologies. Confirmation of site-specific irradiance levels and seasonal and diurnal patterns with on-site measurements is often required during the process of developing project plans and financing arrangements. The high cost of such measurements with typical high quality thermopile irradiance measurement is often a serious impediment to deployment. This effort is an attempt to improve the accuracy of a lower cost direct beam measurement system. This paper describes the approach and elements of the correction to be developed. As of the date of submission of this paper however, only interim correction algorithms are available. Final correction algorithms will be published once additional data collection and refinement is complete in approximately one year.

1. Introduction

Measuring direct normal solar irradiance (DNI) is of great importance in the development of concentrating solar power plants. Accurate DNI measurements reduce uncertainty in predicting plant performance, thus lowering the perceived risk of investment in such projects, facilitating more rapid acceptance and growth of the industry as a whole. However, accurate DNI measurements are costly, both in terms of equipment and maintenance.

The purpose of this investigation is to improve the accuracy of DNI measurements made with a commercially available, low cost system known as the rotating shadow band pyronometer (RSP). This was done using data sets with both a RSP and more accurate, expensive devices (Nip and shaded 8-48). Two data sets were used, one collected by NREL, the other by the University of Oregon Solar Monitoring Laboratory.

A correction algorithm was developed based on previous work by David King of Sandia National Laboratories and Frank Vignola. The first step to correcting the DNI produced by the RSP was to correct the Diffuse Horizontal Solar Insolation (DHI_U). Next accurate solar position values needed to be calculated to correct the Global Horizontal Solar Insolation (GHI_U). The corrected DNI (DNI_C) was then calculated from the corrected Diffuse Horizontal Solar Incidence (DHI_C), the corrected Global Horizontal Solar Incidence (GHI_C), and the accurate solar position values.

2. Normalizing the Data

The LiCor data collected prior to the beginning of the project was recalibrated to eliminate data variations due to calibration differences at the different sites. The ratio of the true global (baseline direct beam multiplied by the cosine of the zenith angle + baseline diffuse) to the measured global was calculated between the zenith angles of 45 and 55 degrees. The average of this ratio is the Calibration Correction Factor. The solar data from the RSP was multiplied by the Calibration Correction Factor to normalize it. The Calibration Correction Factors were 1.03462 and 0.961267 for the NREL and Eugene sites respectively.

Data collected after the project began had no need to be recalibrated as the Li-COR sensors used by the RSP were calibrated at NREL's Solar Radiation Research Laboratory (SRRL).

3. Diffuse Correction

The diffuse measurement was corrected using a combination of two diffuse correction algorithms developed by Frank Vignola[1,2]. For simplicity, the combined correction was called The Vignola Diffuse Correction. The Vignola Diffuse Correction modifies the uncorrected diffuse horizontal irradiance (DHI_U) by a function of the uncorrected global horizontal irradiance (GHI_U). For GHI_U values less than, or equal to, 865.2 W/m^2 equation 1 is used to calculate the corrected diffuse horizontal irradiance (DHI_c); for GHI_U values greater than 865.2 W/m^2 equation 2 is used to calculate the DHI_c :

$$DHI_{C1} = DHI_U + GHI_U * (-9.1*10^{-11} GHI_U^3 + 2.3978*10^{-7} * GHI_U^2 - 2.31329234*10^{-4} * GHI_U + 1.1067578794*10^{-1}) \quad \textbf{(1)}$$

$$DHI_{C2} = DHI_U + GHI_U * (0.0359 - 0.00000554 * GHI_U) \quad \textbf{(2)}$$

The resulting correction is shown in Figure 1.

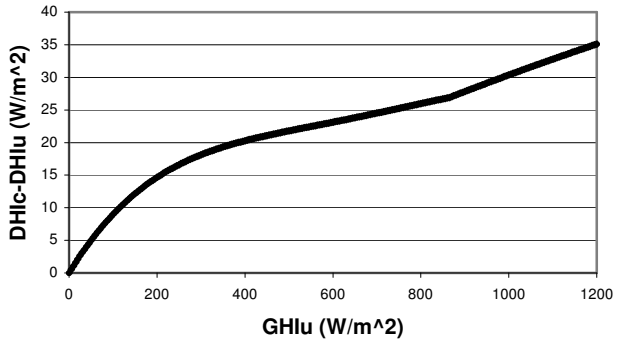

Figure 1: Diffuse Correction, DHI_c -DHI_u

4. Calculating Solar Position

The zenith angle calculation is based on Michalsky's algorithm for approximate solar position[3]. Corrections are made for both air temperature and barometric pressure (approximated by the elevation of the RSP if no data is available). The algorithm replaced the RSP's original algorithm for calculating zenith angle.

Air mass is calculated using the zenith angle, barometric pressure, and an algorithm given by F. Kasten and A. Young[4]. The data logger attached to the RSP calculates the zenith angle and the air mass on the minute.

5. Global Correction

The GHI_u was first corrected using an algorithm developed by David King[5]. The King algorithm has three components, a spectral correction, F_a which is a function of air mass, an angular correction, F_b which is a function of zenith angle, and F_{alpha} which is a function of pyronometer temperature. F_a and F_b are third order polynomials with the following coefficients:

Coef	Value
A0	9.320E-01
A1	5.401E-02
A2	-6.319E-03
A3	2.631E-04
B0	1.000E+00
B1	6.074E-05
B2	1.357E-05
B3	-4.504E-07

Table 1: King algorithm polynomial coefficients

F_{alpha} is of the form: $1-\alpha(T_{pyro} - T_0)$ where α is 0.00082, T_{pyro} is the temperature of the pyronometer, and T_0 is a reference temperature, 25°C.

The King algorithm calculated the corrected global horizontal irradiance (GHI_c) using the following equation:

$$GHI_c = GHI_U * \frac{F_{alpha}}{F_A * F_B} \quad \textbf{Equation 3}$$

At high zenith angles (above 75°), an error was seen in the RSP's global and direct values after applying the Vignola Diffuse Correction and the King Correction. The basis of the error is the geometry of the LiCor. The effect is shown when GHI_c is divided by the baseline global; a spike is present around zenith angle 81°.

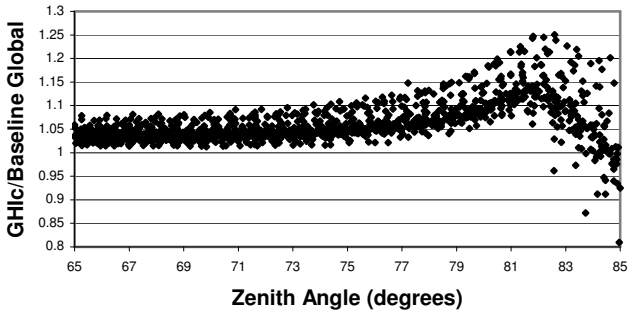

Figure 2: NREL GHI_c/Base Line Global from 65-85° Zenith Angle: The Cat Ear Error.

A new correction algorithm, called the "Cat Ear Correction," was developed to reduce this error. The Cat Ear Correction is two equations, one, Equation 4, applied between zenith angles of 75° and 81°, the other, Equation 5, between 81° and 83.2°.

$$0.001603 * ZA^2 - 0.24242 * ZA + 10.164664 \quad \textbf{(4)}$$

$$-0.00899 * ZA^2 + 1.457577 * ZA - 58.03442 \quad \textbf{(5)}$$

where ZA is the zenith angle in degrees. The combination of the two equations is shown in Figure 3:

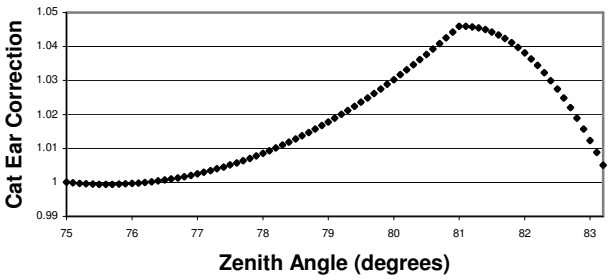

Figure 3: Cat Ear Correction

The combination of the King Correction and the Cat Ear correction is what was used to correct the global horizontal irradiance, given by equation 6.

$$GHI_C = GHI_U * \frac{F_\alpha}{F_A * F_B * F_C} \qquad \textbf{Equation 6}$$

where F_c is the Cat Ear Correction.

7. Results

Comparing the ratios of the measured and corrected data to the respective baseline data shows the effectiveness of the correction algorithm. In the ideal case, the corrected data would equal one after this operation. The standard deviation of the data gives the correction algorithm one measure of goodness. The standard deviation is calculated using equation 7 where y is the measured value, y(x) is the mean value and n is the number of measurements.

$$sd = \sqrt{\frac{\sum_{i=1}^{n} (y(x) - y)^2}{n}} \qquad \textbf{Equation 7}$$

Another measure of goodness is the mean. The mean distinguishes between systematic and random error. The closer the average is to 1, the closer the data is to the baseline.

To evaluate the effectiveness of the correction algorithm, both the average and the standard deviation need to be considered. Table 2 gives the average and standard deviation of corrected and uncorrected data:

Measurement	Standard Deviation		Average	
	Uncorrected	Corrected	Uncorrected	Corrected
Global	0.024111	0.019476	0.996401	0.990582
Direct	0.042607	0.03185	1.050311	0.983107
Diffuse	0.065247	0.046875	0.653496	1.027903

Table 2: Results of Applying Correction Algorithm

The effect of the correction algorithm on the measured data can be seen by looking at plots of the measured data divided by the baseline data compared to the corrected data divided by the baseline data on a typical clear day. Figure 4 is a plot of the measured diffuse, DM2D, and the corrected diffuse, DV2D, both divided by the baseline:

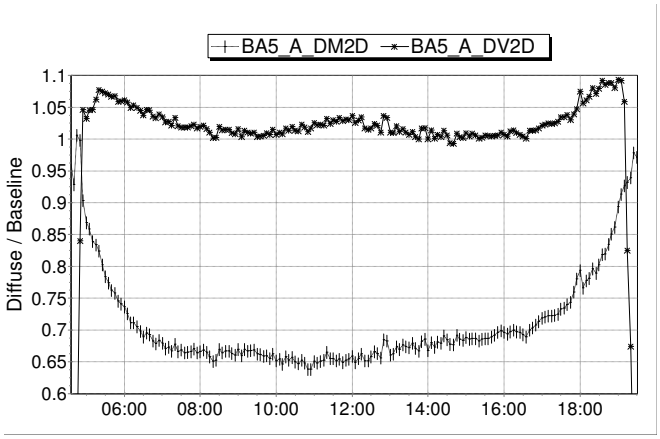

Figure 4: DM2D and DV2D on a Typical Clear Day

Figure 5 shows the measured global, GM2G, compared to the corrected global, GVKC2G, both divided by the baseline:

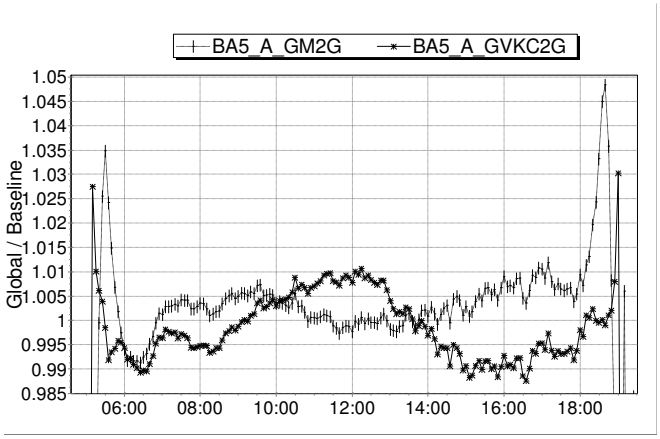

Figure 5: GM2G and GVKC2G on a Typical Clear Day

Figure 6 shows the measured direct beam, BM2B, compared to the corrected direct beam, BVKC2B, both divided by the baseline:

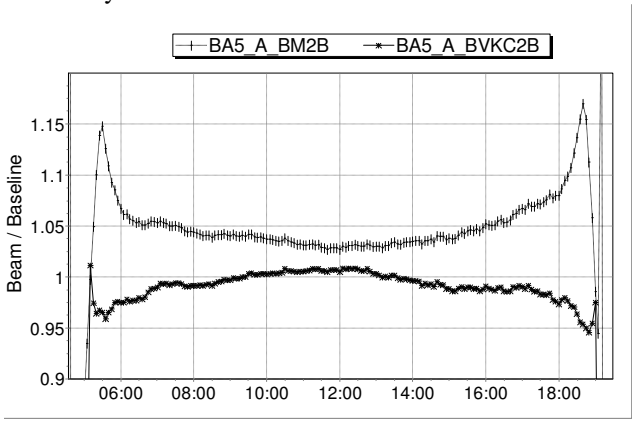

Figure 6: BM2B and BVKC2B on a Typical Clear Day

Looking at the direct beam and global data between the zenith angles of 75 and 83.2 degrees can see the effectiveness of the Cat Ear correction. Table 3 gives the

average and standard deviation of data corrected with and without the Cat Ear correction:

Measurement	Standard Deviation		Average	
	With CE	Without CE	With CE	Without CE
Global	0.038447	0.042722	0.999711	1.017801
Direct Beam	0.07077	0.071822	0.976634	1.001595

Table 3: Comparison of Global and Direct Beam data corrected With and Without the Cat Ear Correction between Zenith Angles 75 and 83.2 Degrees

Figure 7 shows the corrected direct beam with and without the Cat Ear correction, divided by the baseline, on a typical clear day:

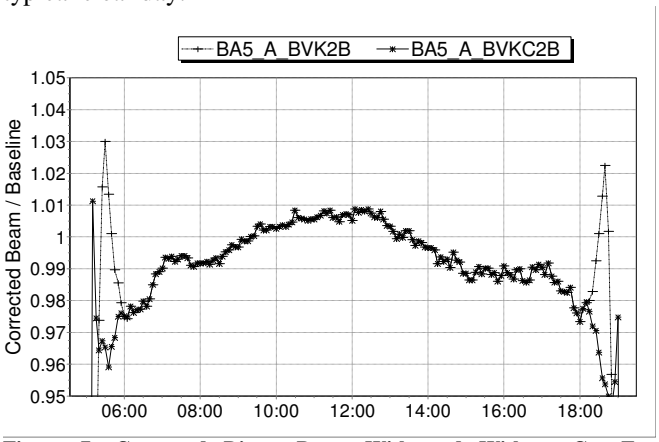

Figure 7: Corrected Direct Beam With and Without Cat Ear Correction

Figure 8 shows the corrected global with and without the Cat Ear correction, divided by the baseline, on a typical clear day.

Figure 8: Corrected Global With and Without Cat Ear Correction

8. Discussion

The primary goal of this project was to improve the accuracy of the RSP's direct beam measurement. This was done through three different corrections: zenith angle, diffuse, and global. The standard deviation of the direct beam measurement was reduced from 0.042607 to 0.03185 and the average value of the direct beam measurement was reduced from 1.050311 to 0.983107.

These results show an improvement both in the systematic and random error. The reduction in the standard deviation show the scatter of the DNI measurement being reduced; the mean of the data approaching unity shows a stronger correlation between the measured data and the baseline data.

The improvement to the direct beam measurement can be demonstrated by considering the error that is expected before and after the correction. Before the correction, the data could be expected to be 5% greater than the true value, +/- 8%. On a clear day, this could mean an error of over 130 W/m^2. After the correction, the data could be expected to be 1.7% low, +/- 6%, of true, reducing the error on a clear day by 60 or 70 W/m^2.

The greatest error occurs at low zenith angles, as can be seen in figures 6 and 7. The Cat Ear correction is an attempt to solve this problem. The standard deviation of the direct beam with the Cat Ear correction is less than the standard deviation of the direct beam without the Cat Ear correction, but not by much. The average of the direct beam deviated further from unity when the Cat Ear correction was applied. however, the average did approach the average of the over all corrected direct beam, suggesting that the Cat Ear correction is improving the accuracy of the direct beam measurement, but there is a systematic error independent of the Cat Ear correction.

This raises the question of what causes the systematic error in the direct beam data. To see the effect of the zenith angle calculation the corrected direct beam on a horizontal surface (DHS) can be compared to the baseline DHS. The DHS is calculated by subtracting the diffuse from the global irradiance. The corrected DHS divided by the baseline DHS had a standard deviation of 0.03603295 and an average of 0.983107. Figure 9 shows the distribution of the corrected DHS divided by the baseline DHS over a range of zenith angles.

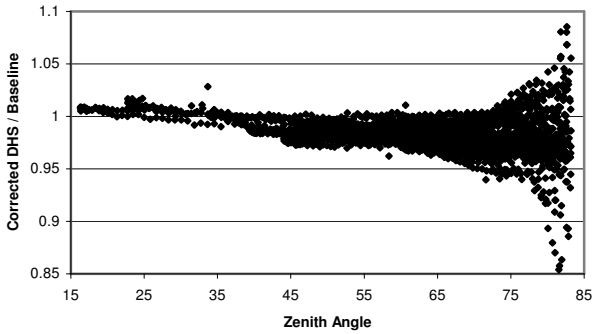

Figure 9: Corrected Direct Beam Projected on a Horizontal Surface Divided by Baseline Over a Range of Zenith Angles

The standard deviation and average of the corrected DHS is close to the values for the corrected direct beam. Both have

an average less than one, and a similar standard deviation. This indicates that the systematic error is in the measurement or correction of the irradiance values and not in the calculation of the zenith angle.

9.Conclusion

Low cost direct beam measurements can be made more accurate through the use of a set of algorithms based on GHI, DHI, and the solar position. The correction to the RSP diffuse measurement has the greatest effect on improving accurate DNI estimates. At very high zenith angles, corresponding to periods of plant start up and shut down, significant improvement can be realized with a simple two part regression model.

Final correction algorithms will be developed after additional data are collected at additional sites.

---

[1] Vignola, Frank. Solar Cell Based Pyronometers: Evaluation of the Diffuse Response, *Proceedings of the 1999 Annual Conference, American Solar Energy Society,* 260, June 1999.

[2] Vignola, Frank. Direct correspondence.

[3] Michalsky, Joseph. The Astronomical Almanac's Algorithm for Approximate Solar Position (1950-2050), *Solar Energy* **40**, 227 (1988).

[4] Kasten, F. and Young, A. Revised Optical Air Mass Tables and Approximation Formula, *Applied Optics* **28**, 4735 (1989).

[5] King, David L., Boyson, William E., and Hansen, Barry R. Improved Accuracy for Low-Cost Solar Irradiance Sensors, *Presented at 2nd World Conference and Exhibition on Photovoltaic Solar Energy Conversion,* July 6-10, 1998.